IEEE Access
Multidisciplinary ⋮ Rapid Review ⋮ Open Access Journal

Received 14 October 2024, accepted 8 November 2024, date of publication 12 November 2024, date of current version 22 November 2024.

Digital Object Identifier 10.1109/ACCESS.2024.3496510

RESEARCH ARTICLE

Jump Rope Exercise Assistance Program

JIN-WOONG KIM[1], JAE-WOO SHIN[2], AND SEOUNG-HO CHOI[3]
[1]Department of Convergence IT Engineering, Hansung University, Seoul 02876, South Korea
[2]Department of IT Business Admiration, Hanshin University, Osan-si, Gyeonggi-do 18101, Republic of Korea
[3]College of Liberal Arts, Faculty of Basic Liberal Arts, Hansung University, Seoul 02876, South Korea

Corresponding author: Seoung-Ho Choi (jcn99250@naver.com)

This work was supported by Hansung University.

This work involved human subjects or animals in its research. The authors confirm that all human/animal subject research procedures and protocols are exempt from review board approval.

ABSTRACT Jump rope exercise requires a fast tempo and breathing, which often leads to the problem of users forgetting their jump count during the workout. To address this issue, we propose a jump rope exercise assistance program that recognizes the user's jump rope motions and analyzes the impact of joint coordinates on these motions. The proposed solution extracts frame-by-frame joint coordinate data from jump rope performance videos. It then utilizes artificial intelligence models to recognize jump rope motions and measure the jump count through motion recognition. We employed five machine learning models and two deep learning models to validate the jump rope motion recognition and count measurement. We analyzed the joint coordinates significantly influencing each jump rope motion using SHAP. Furthermore, we used Odds Ratios to analyze the jump rope motion occurrence probability based on joint coordinate values. Through these methods, we confirmed that the proposed solution effectively performs jump rope motion recognition and joint coordinate impact analysis for jump rope motions.

INDEX TERMS Exercise assistance program, artificial intelligence, jump rope recognition, jump rope factor analysis, jump rope odd ratio.

I. INTRODUCTION

Jump rope has been scientifically proven to provide exercise benefits comparable to aerobics. It is a sport that enhances motor skills such as strength, speed, agility, coordination, timing, and rhythmic sense while promoting overall physical health [1]. Moreover, it is a versatile sport that can be conducted regardless of location, number of participants, or gender, making it suitable for leisure activities, individual or group exercises, and recreational or entertainment purposes. Jump rope is easily accessible to anyone because it is easy to obtain equipment and does not require special attire or facilities. Additionally, since jump rope does not involve sudden movements or collisions with other players, the risk of serious injury is extremely low, a significant advantage of this exercise form [2].

The associate editor coordinating the review of this manuscript and approving it for publication was Muammar Muhammad Kabir.

While jump rope is a sport that involves the repetitive action of turning a rope and jumping, it is one of the high intensity aerobic exercises that aid in weight loss [1]. For this reason, many individuals have been contacted with jump rope from childhood, and it is not uncommon to find adults performing jump rope for aesthetic purposes.

Because jump rope requires fast tempo and breathing, it is often not easy to accurately count the number of jumps while focusing on fast movements. Furthermore, as one engages in jump rope for extended periods, the motion becomes automated, making it increasingly difficult to consciously count the number of jumps. Also, as one engages in jump rope for extended periods, the motion becomes automated, making it increasingly difficult to consciously keep track of the count. For this reason, individuals often experience difficulty in maintaining an accurate tally of their jumps. When individuals are unable to accurately count the number of jumps during jump rope, the following issues may arise. Firstly, there is a reduction in exercise effectiveness. Without

precise knowledge of the appropriate number of jumps for oneself, it becomes challenging to properly adjust the intensity and duration of the exercise. Secondly, there is an increased risk of injury. Failure to accurately determine the suitable number of jumps can lead to excessive exercise, potentially elevating the risk of injury. Thirdly, there is a decrease in motivation due to difficulties in maintaining accurate records. The inability to precisely record one's jump count may result in diminished motivation for exercise. To address these issues, this study proposes a program that utilizes video analysis methods to extract frame-by-frame joint coordinate data from jump rope performance videos and measures the jump count. Video analysis is cost-effective and applicable in various exercise environments without the need for equipment like smartwatches. It allows for precise measurement and analysis of jump rope movements, helping users effectively understand their exercise patterns. Previous studies have proposed various approaches for recognizing athletic movements; however, many of these approaches do not provide real-time feedback or have limitations in applicability across diverse environments. These limitations include a lack of real-time feedback and restricted applicability in various settings. In consideration of these challenges, this study focuses on recognizing each jump rope movement through video analysis and analyzing the impact of joint coordinates on these movements. The contributions of this paper are as follows:

- We propose an assistive program for jump rope exercises that recognizes the user's jump rope movements and analyzes the impact of joint coordinates on these movements.
- To recognize jump rope movements and measure the number of jumps, we conducted validation using five machine learning models and two deep learning models.
- We enhanced the accuracy of jump count measurements by applying a moving average technique to reduce noise, resulting in smoother and more reliable predictions.
- We analyzed the joint coordinates that influence each jump rope movement using SHAP. Additionally, we used Odds Ratio analysis to determine which joint coordinate values increase the probability of executing jump rope movements.
- We confirmed that the proposed solution effectively performs the recognition of jump movements and the analysis of joint coordinate influences on these movements.

The remainder of this paper is structured as follows. Section II explains the background theory used for measuring the number of jump repetitions. Section III describes previous research similar to our proposed jump rope assistive solution for jump rope exercises. Section IV describes our proposed method, including information on the dataset and models and analysis techniques used. Section V describes the experimental methodology, including evaluation metrics and model training. Section VI and VII describe the experimental results and discussion, respectively. Finally, Section VIII concludes the paper by summarizing our findings and contributions.

II. BACKGROUND THEORY

Openpose is a technique within the field of Human Pose Estimation that accurately predicts a person's body, face, and finger joints using only a single camera. This technology is designating key points for joints and critical body parts from an image of a person and estimating the positions of body parts, facial features, and finger joints by identifying these key points in the human image [3]. Before openpose, a Top-Down approach was employed, which first detects humans and then repeatedly identifies the joint key points of the detected humans. Openpose employs a Bottom-Up approach that operates without the need for repetitive processing. The Bottom-Up approach first estimates all joint key points present in the body and then groups these key points into specific poses or the pose of a single person. It is easy to apply in real time because it does not go through the process of detecting people first. Recently, the One-Shot method, which is an evolution of the Bottom-Up method, was proposed. The One-Shot method is a method of predicting the distance between each joint from the center based on the position of the center. It has the advantage of being a very fast inference speed because it does not require a grouping process that requires optimization [4].

CNN models provided by Openpose include Body25, COCO, and MPII. Body25 has 25 output joints, COCO has 18 output joints, and MPII has 15 output joints. There is a difference in the number of joints extracted between each model.

III. RELATED WORK

Various methods are used to measure the number of jumps performed. There are two methods: measuring method the number of jumps performed using a smartwatch and measuring method the number of jumps performed using a count jump rope.

Most smartwatches use accelerometer and gyroscope sensors to measure the number of jumps performed [5], [6], [7]. The accelerometer measures the acceleration of the device to which the sensor is attached, and the gyroscope sensor measures the rotation speed of the device to which the sensor is attached. During the jump rope activity, when the arms go down, the acceleration increases significantly under the influence of gravity, and when the arms go up again, the acceleration decreases due to gravity. The number of jumps performed is measured by analyzing the acceleration change pattern of the device measured using an accelerometer. Gyroscope sensors detect angular velocity, that is, rotational speed and direction of rotation. Each time the arm rotates during a jump rope activity, the number of times the arm rotates is calculated based on the rotation speed and direction of rotation to measure the number of jumps performed. Count jump rope measures the number of jumps performed by embedding a gear-like sensing device in the handle and then

increasing the counter on the handle by 1 by turning the gear as the rope rotates.

Kim et al. [8] proposed a motion similarity measurement program through skeleton image binarization. To calculate the overlap range, they extracted the skeleton images frame by frame from the input user's exercise image and reference image, and then converted them to a binary image. Afterward, operation processing is performed on the reference image converted to a binary image and the user's exercise image, and the accuracy of the exercise posture is calculated based on the overlapping range of the reference image and the user's exercise image and provided to the user, allowing the user to exercise in the correct posture.

Kim et al. [9] proposed a program that uses the Unet model and open poses to find areas that require exercise posture correction and provide them to the user. They used the user's exercise video as input to the Openpose model to extract key points and then used them as input to the exercise posture analysis model using the U-Net deep learning architecture. Afterward, the angles between key points such as upper body position, elbow angle, arm position, and posture completeness are calculated and compared with the reference image to find areas requiring posture correction and provide the information to the user. The conclusion was drawn that the user's exercise posture can be recognized and corrected using only the Unet model and openpose.

Choi et al. [10] proposed a deep learning-based algorithm that collects user exercise data through the IMU sensor built into the hearing device and uses it to predict exercise type and number of repetitions. To improve the prediction performance of the proposed algorithm, data augmentation techniques such as noise injection, time warping, and split and merge were applied to the collected sensor time series data. The experiment compared performance in three scenarios: without augmentation techniques, with each augmentation technique applied individually, and with all augmentation techniques experimental results applied together. The confirmed that the highest performance was achieved when all three augmentation techniques were applied to the sensor time series data.

Lee et al. [11] proposed an algorithm that evaluates the exercise movement state and detects incorrect movement using only Openpose. They extracted a total of 50 coordinates using the Body25 model, which extracts 25 joint keypoints. The experiment was conducted in a manner that compared the joint angle information obtained from these coordinates with the predetermined coordinate ranges in real-time. The experimental results concluded that most exercise states could be accurately assessed, and incorrect exercise movements detected, using only the x and y coordinates obtained from video detection.

Previous studies have proposed various approaches for recognizing athletic movements, but they have some limitations. Kim et al. evaluated the accuracy of exercise posture through skeleton image binarization; however, this method does not allow for real-time analysis and does not provide immediate feedback to the user. In the study by Choi et al., an IMU sensor was used to predict exercise type and repetition counts. Still, the necessity of sensor equipment incurs additional costs and limits applicability in various exercise environments. Lee et al. utilized OpenPose to assess exercise status, yet this also does not provide real-time feedback and faces challenges in detecting incorrect movements. Thus, existing research presents challenges in delivering real-time feedback, incurs additional costs, and is limited in applicability across different exercise settings. These issues highlight the need for alternative approaches that can effectively recognize athletic movements while addressing these limitations.

IV. PROPOSED METHODOLOGY

We propose a jump rope motion assistance solution that recognizes the user's jump rope motion and analyzes the effect of joint coordinates on the jump rope performance.

The overall system structure of the proposed program is depicted in Fig. 1. The proposed jump rope exercise assistance program first collects videos of two types of jump rope movements (single jump and double jump) performed by ten individual users. It then utilizes the MPII model of the OpenPose library to extract joint coordinates frame by frame from the collected videos. During this process, the extracted joint coordinate data from each frame is saved in CSV format, with the last column of each CSV file labeled as 0 when the foot is on the ground and as 1 when the foot is in the air. Min-Max scaling is applied to the extracted joint coordinate data, and missing values are replaced with the average of the joint coordinates from the previous and next frames to maintain data continuity. Afterward, Pearson correlation analysis is conducted to examine the correlation of each joint coordinate with the jump rope movements.

To recognize jump rope movements and measure the number of repetitions, we train and evaluate a total of seven classification models: Random Forest, Extra Trees, CatBoost, LightGBM, XGBoost, LSTM, and Transformer. The performance of each model is assessed comprehensively based on accuracy, precision, recall, F1 score, AUROC, and average precision.

The number of jump rope repetitions is counted each time the label value transitions from 0 to 1. The distribution of label values typically exhibits a sequence where a series of 0s and 1s appear repeatedly. Consequently, even a single noise introduced in the predicted values can significantly alter the count of jump rope repetitions. To address this issue, we propose applying the moving average technique to the predicted values to reduce noise and enhance the accuracy of the results. The process of applying the moving average is visualized in Fig. 2. After applying a moving average with a window size of 5 to the model's predictions, rounding is performed on each value to obtain integer values of either 0 or 1. This process reduces the noise in the jump count predictions of the model, where label values appear consecutively as 0 or 1, thereby improving the accuracy of the jump count prediction. The moving average is computed

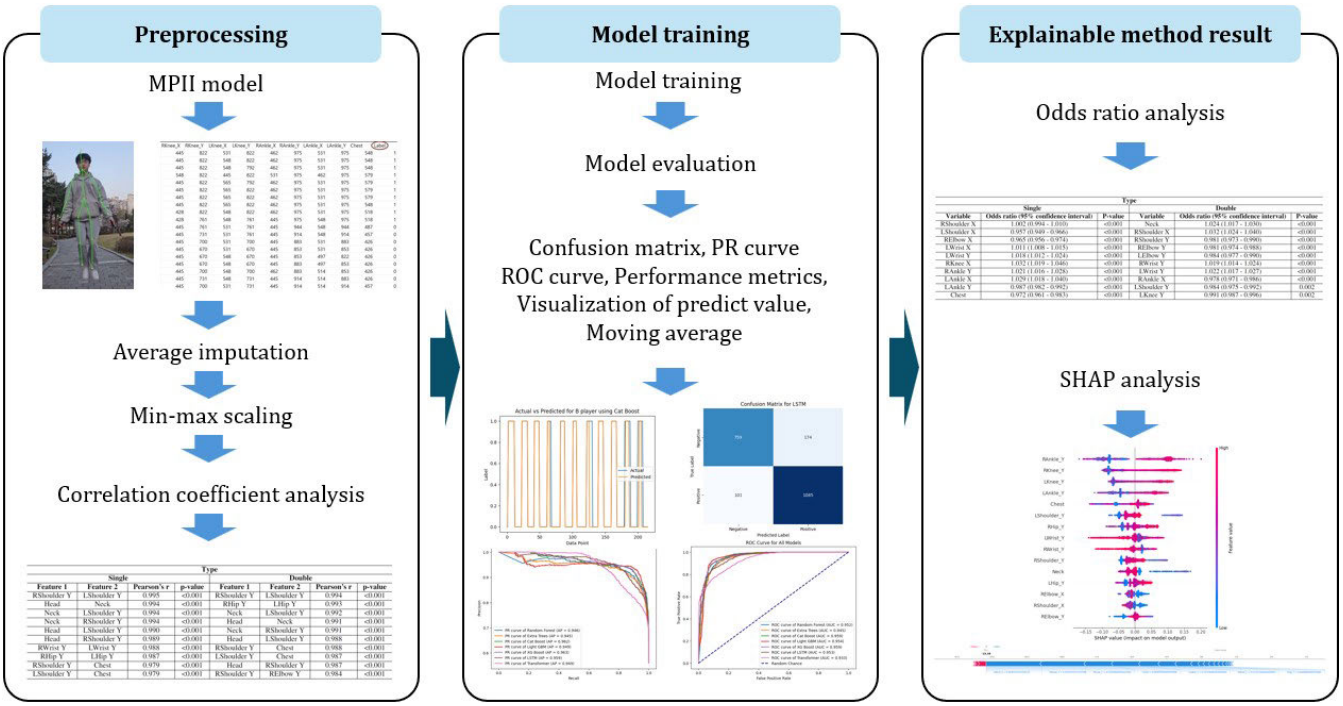

FIGURE 1. Our proposal.

using the following equation:

$$\mathrm{MA}(y, M) = \mathrm{round}\left(\frac{1}{M}\sum_{i=0}^{M-1} y_{t-i}\right) \tag{1}$$

In equation (1), y_t represents the prediction at time t, and M denotes the window size. By applying this method, we can smooth the prediction results, allowing for a more accurate estimation of the number of jump rope repetitions. This equation computes the moving average by averaging the most recent M predictions and replacing the corresponding M values with the rounded average. This process reduces fluctuations in the prediction values and provides a more stable estimate.

Additionally, evaluation metrics such as ROC curves, PR curves, confusion matrices, and visualizations of the model's prediction results are included to analyze the model's performance from multiple perspectives. Finally, we perform an odds ratio analysis for each joint coordinate to compare the probabilities of the foot being on the ground (0) and in the air (1) during jump rope movements. Moreover, SHAP analysis is conducted to interpret the prediction results of the best-performing model and analyze the impact of joint coordinates on jump rope performance.

V. EXPERIMENTAL METHODOLOGY

We was conducted under conditions that did not require ethics approval. The study was conducted on human participants, and all participants gave verbal consent after the purpose and procedures of the study were fully explained. The data used in the study was used for analysis by extracting only the joint coordinates from the participants' rope jumping exercises, no personally identifiable information was collected, and the videos used in the experiment were safely deleted to protect personal information. Considering the differences in jump periods and movements among the jump rope performers, we recruited 10 performers and directly recorded the videos to collect data for training. Each performer completed 3, 5, 7, 9, and 11 repetitions of both single and double types of jumps, resulting in a total of 100 jump rope performance videos. We extracted joint coordinate data for each frame from the jump rope performance video using the MPII model. We extracted joint coordinate data for each frame from a total of 100 jump rope performance videos taken by 10 motion performers, each of which was saved as a CSV file. As a result of the extraction, a CSV file was generated that stored a total of 100 joint coordinate data, 10 per person performing the jump rope motion. For each jump rope performance video, an average of about 150 frames were extracted in proportion to the number of jump performances. All joint coordinate data values of parts where the jump rope was not performed, such as before starting and after ending the jump rope, or parts that could not be performed in the middle, were removed and processed to make it suitable for use. Additionally, to use the data as training input, the point when the foot touches the ground was labeled as 0, while other sections were labeled as 1, and the data was added in the last column of each CSV file. The labeled CSV file image is depicted in Fig. 2.

Missing values that occurred during the extraction of joint coordinate data for each frame were replaced with

RKnee_X	RKnee_Y	LKnee_X	LKnee_Y	RAnkle_X	RAnkle_Y	LAnkle_X	LAnkle_Y	Chest	Label
445	822	531	822	462	975	531	975	548	1
445	822	548	822	462	975	531	975	548	1
445	822	548	792	462	975	531	975	548	1
548	822	445	822	531	975	462	975	579	1
445	822	565	792	462	975	531	975	579	1
445	822	565	822	462	975	531	975	579	1
445	822	565	822	462	975	531	975	579	1
445	822	565	822	462	975	531	975	548	1
428	822	548	822	462	975	531	975	518	1
428	761	548	761	445	975	548	975	518	1
445	761	531	761	445	944	548	944	487	0
445	731	531	761	445	914	548	914	457	0
445	700	531	700	445	883	531	883	426	0
445	670	531	670	445	853	531	853	426	0
445	670	548	670	445	853	497	822	426	0
445	670	548	670	445	883	497	853	426	0
445	700	548	700	462	883	514	853	426	0
445	731	548	731	445	914	514	883	426	0
445	700	531	731	445	914	514	914	457	0

FIGURE 2. Labeling example for the jump rope dataset.

the average of the previous and next frames' values for the corresponding joint. Additionally, Min-Max Scaling was applied to normalize the joint coordinate data between 0 and 1, ensuring that no feature dominated the training process. The 100 joint coordinate data CSV files were split 6:2:2 for training, validation, and testing. During this process, shuffle was not applied to preserve the time-series characteristics of the dataset. Finally, the divided CSV files were merged for training.

We calculated the Pearson correlation coefficient to analyze the relationships between joint coordinates during jump rope execution. This analysis allowed us to quantitatively assess the impact of the movement of specific joints on other joints. The Pearson correlation coefficient is suitable for measuring the linear relationship between two variables and is particularly useful for the joint coordinates of jump rope movements, which typically represent continuous values. We focused on calculating the correlation coefficients for each pair of joint coordinates to identify significant linear relationships among continuous variables. The Pearson correlation coefficient takes values between -1 and 1, where values close to -1 indicate a negative correlation, values close to 1 indicate a positive correlation, and values close to 0 indicate little to no correlation [12]. Additionally, this analysis was performed separately for single and double jump rope data within the training dataset, providing valuable insights for a clearer understanding of how the movement of specific joints affects the movements of other joints.

To analyze joint coordinate data extracted from jump rope performance videos, we employ five tree-based machine learning models including Random Forest, Extremely Randomized Trees (Extra Trees), Categorical Boosting (Cat Boost), Light Gradient Boosting Machine (Light GBM), and Extreme Gradient Boosting (XG Boost), as well as two deep learning models, Long Short-Term Memory (LSTM) and Transformer. Tree-based models are well-suited for handling structured data and perform excellently even with high-dimensional datasets. In particular, tree-based ensemble methods effectively capture nonlinear relationships and interactions between variables [16], [17]. Conversely, LSTM and Transformer models excel at capturing sequences and long-term dependencies, demonstrating high performance with time-series data or data with temporal structures [18], [19]. For these reasons, we have determined that these models are appropriate for analyzing joint coordinate data extracted from jump rope performance videos and use them for predicting key metrics related to jump rope execution.

Random Forest is a method that improves prediction performance by aggregating multiple decision trees. Each tree is generated using a set of variables through bootstrap sampling and feature bagging. The final prediction result is obtained by averaging or voting on the predictions of all trees. This approach is effective in preventing overfitting and enhancing the generalization performance of the model [13].

Extra Trees is an ensemble method similar to Random Forest but includes more randomness in the model training process. While Random Forest finds the optimal split at each node, Extra Trees uses randomly chosen split criteria to build the trees. This may slightly increase the model's bias but reduces variance, which helps in preventing overfitting [14].

Cat Boost is a gradient boosting library developed by Yandex that effectively handles categorical data. The algorithm adopted an Ordered Boosting technique to prevent overfitting and enhance the model's generalization performance. Additionally, CatBoost provides optimized implementations for efficient training and prediction, demonstrating excellent performance even on large datasets and complex problems [15].

Light GBM is a Gradient Boosting technique developed by Microsoft, designed to work efficiently on large-scale data and in high-dimensional spaces. Unlike GBM and XG Boost, which use a level-wise approach, Light GBM employs a leaf-wise approach, splitting the leaf node with the maximum loss to create deep and asymmetric trees. It also significantly accelerates the training rate by using techniques like Gradient-based One-Side Sampling(GOSS) and Exclusive Feature Bundling (EFB) [16].

XG Boost enhances the efficiency and performance of Gradient Boosting by refining the algorithm and optimizing system design. It improves training speed and the model's generalization performance through regularization, parallel processing, and pruning with a specified maximum depth. However, it has limitations, such as high memory usage and lower performance on imbalanced data [17].

The LSTM model is a type of recurrent neural network (RNN) designed to address the long-term dependency problem that occurs when dealing with sequence data. RNNs use information from previous time steps to make predictions for the next time steps. However, in long sequences, the information from earlier time steps tends to diminish over time, leading to the vanishing gradient problem, which makes learning difficult. The LSTM model overcomes this issue by introducing a structure with a cell state and gates, allowing it to selectively retain or forget information. This enables LSTM to effectively learn from long sequences while preserving important information. As a result, LSTM is

widely used in various fields such as time series forecasting, natural language processing, and speech recognition [18].

The Transformer model is an artificial neural network designed to handle sequential data, but unlike traditional RNNs or LSTM models, it does not require sequential processing and can handle data in parallel. This greatly improves training speed, making it particularly advantageous for working with long sequences. The core of the Transformer model is the self-attention mechanism, which simultaneously considers the relationships between all elements in a sequence to better understand the context. Due to these features, the Transformer model is widely used in various fields such as time series forecasting, natural language processing, and machine translation [19]. For the five machine learning models, we tuned the optimal hyperparameters using grid search. During the training of the LSTM model, two LSTM layers and two dropout layers were used, and a dense layer was applied as the output layer. For the binary classification task, the Sigmoid function was chosen as the activation function for the output layer. We used the Adam optimizer and employed binary cross-entropy as the loss function. The learning rate was set to 0.001, and the number of epochs was set to 100. The Transformer model consists of two transformer blocks, with the Sigmoid function also used as the activation function for the output layer. Dropout rates of 0.25 and 0.4 were applied to the multi-head attention and MLP layers, respectively. The optimizer used was Adam, and the loss function selected was binary cross-entropy. The learning rate was set to 0.001, with a batch size of 32 and 100 epochs for training.

Performance evaluation was conducted by visualizing Accuracy, Precision, Recall, F1 Score, AUROC, and Average Precision. The equations for each performance evaluation metric are as follows.

$$\text{Accuracy} = \frac{TP + TN}{TP + TN + FP + FN} \tag{2}$$

$$\text{Precision} = \frac{TP}{TP + FP} \tag{3}$$

$$\text{Recall} = \frac{TP}{TP + FN} \tag{4}$$

$$\text{F1 Score} = 2 \times \frac{\text{Precision} \times \text{Recall}}{\text{Precision} + \text{Recall}} \tag{5}$$

$$\text{AUROC} = \int_0^1 \text{TPR}(x)\, d(\text{FPR}(x)) \tag{6}$$

$$\text{AP} = \sum_n (R_n - R_{n-1})\, P_n \tag{7}$$

In the above Equation (2)-(7), TP is True Positive, meaning that the model correctly classifies data that is positive as positive. TN is True Negative, meaning that the model correctly classified data that is actually negative as negative. FP is False Positive, meaning that the model incorrectly classified data that is actually negative as positive. FN is False Negative, meaning that the model incorrectly classifies data that is actually positive as negative. Equation (2) represents the proportion of correctly predicted instances across the entire dataset. Accuracy is an overall performance metric for the model, but it has the limitation of not providing an accurate evaluation when there is an imbalance in class distributions. Equation (3) represents the proportion of what the model predicts as True that is actually True. High precision means that most of the data predicted by the model as True is actually True. Equation (4) represents the ratio of data predicted as True by the model among data that is actually True. A higher recall means that the model is better at identifying data that is actually true. Equation (5) represents the F1 Score, which is calculated as the harmonic mean of Precision and Recall. It serves as a comprehensive performance metric that balances both Precision and Recall. The F1 Score is particularly useful for evaluating model performance on imbalanced datasets. In Equation (6), TPR (True Positive Rate) is equivalent to Recall. FPR (False Positive Rate) indicates the proportion of actual negative cases that are incorrectly classified as positive by the model. The ROC Curve illustrates the relationship between TPR and FPR. The AUROC represents the area under the ROC Curve and reflects the overall performance of the model. In Equation (7), $P_n$represents the Precision at the n-th threshold, and R_n represents the Recall at the n-th threshold. Average Precision indicates the area under the Precision-Recall curve and is calculated using Precision and Recall values at multiple thresholds. A higher AP value indicates that the model performs well in predicting the positive class across various thresholds.

The number of jumps performed is measured by counting each time the label value changes from 0 to 1. However, if noise occurs in the model's predicted values, a large error occurs in the process of measuring the number of jumps performed. To solve this problem, the number of jump repetitions performed by applying the moving average method was predicted. Moving average is a technique used to reduce the volatility of time series data and identify trends more clearly. Moving average works by calculating the average in a specific section of data and reducing noise in the predicted value.

The odds ratio analysis is a statistical method that compares the incidence rates between two groups to evaluate the likelihood of a specific event occurring [20]. To evaluate the impact of joint coordinates on foot position during jump rope performance, we conducted an odds ratio analysis using a logistic regression model. We constructed a dataset by labeling the foot position based on joint coordinate data, where the label was set to 0 when the foot was on the ground and 1 when it was in the air. This approach allowed us to compare the incidence rates between the two states and assess the likelihood of the foot being in the air or on the ground. In the logistic regression model, the dependent variable was the foot position (0 or 1), while the independent variables were the joint coordinate data. After constructing the model, we extracted the odds ratios based on the regression coefficients, enabling us to analyze

TABLE 1. Summary of mean values and standard deviations by label in the jump rope dataset.

Type	Single			Double		
Variables	Feet touching the ground (n = 1,641)	Feet floating in the air (n = 1,269)	P-value	Feet touching the ground (n = 1,471)	Feet floating in the air (n = 1,788)	P-value
Head, mean (SD)	626.7 (150.2)	485.0 (192.6)	<0.001	668.3 (152.8)	559.2 (196.2)	<0.001
Neck, mean (SD)	780.8 (131.3)	646.7 (168.9)	<0.001	816.4 (137.5)	711.3 (177.0)	<0.001
RShoulder X, mean (SD)	511.3 (96.8)	472.3 (87.2)	<0.001	502.9 (91.1)	493.0 (82.9)	0.001
RShoulder Y, mean (SD)	814.6 (114.2)	688.1 (150.9)	<0.001	831.1 (130.9)	723.6 (166.2)	<0.001
LShoulder X, mean (SD)	562.0 (68.7)	581.0 (61.9)	<0.001	578.5 (66.3)	584.5 (70.5)	0.013
LShoulder Y, mean (SD)	812.1 (117.0)	684.8 (154.4)	<0.001	825.6 (132.3)	719.8 (170.0)	<0.001
RElbow X, mean (SD)	511.9 (138.6)	443.4 (119.8)	<0.001	481.9 (126.4)	466.2 (108.8)	<0.001
RElbow Y, mean (SD)	917.0 (88.3)	799.7 (130.1)	<0.001	911.1 (119.4)	811.9 (152.8)	<0.001
LElbow X, mean (SD)	570.0 (110.8)	612.5 (90.2)	<0.001	602.8 (104.3)	608.8 (103.2)	0.098
LElbow Y, mean (SD)	912.8 (95.5)	792.4 (137.1)	<0.001	907.0 (120.2)	813.9 (152.1)	<0.001
RWrist X, mean (SD)	505.1 (181.3)	399.4 (166.0)	<0.001	462.1 (164.8)	432.8 (142.6)	<0.001
RWrist Y, mean (SD)	939.2 (90.4)	830.5 (168.7)	<0.001	914.2 (138.2)	858.4 (166.8)	<0.001
LWrist X, mean (SD)	567.2 (157.8)	651.1 (137.4)	<0.001	615.8 (142.1)	632.0 (143.3)	0.001
LWrist Y, mean (SD)	932.5 (98.2)	819.4 (179.8)	<0.001	912.6 (140.0)	858.9 (174.0)	<0.001
RHip X, mean (SD)	527.3 (57.5)	503.0 (56.2)	<0.001	522.8 (67.5)	516.3 (60.6)	0.004
RHip Y, mean (SD)	1051.5 (77.9)	929.8 (87.8)	<0.001	1042.5 (99.2)	924.9 (125.4)	<0.001
LHip X, mean (SD)	551.7 (41.7)	560.2 (40.2)	<0.001	562.0 (57.2)	561.3 (54.1)	0.745
LHip Y, mean (SD)	1051.1 (81.4)	924.8 (92.5)	<0.001	1039.8 (100.9)	924.8 (126.6)	<0.001
RKnee X, mean (SD)	532.5 (59.9)	507.8 (56.0)	<0.001	526.3 (70.4)	521.4 (64.1)	0.037
RKnee Y, mean (SD)	1192.7 (77.3)	1106.0 (67.6)	<0.001	1169.8 (94.9)	1041.5 (96.5)	<0.001
LKnee X, mean (SD)	559.9 (41.3)	569.2 (38.7)	<0.001	569.0 (55.3)	573.2 (54.2)	0.028
LKnee Y, mean (SD)	1192.3 (74.3)	1101.4 (66.6)	<0.001	1167.8 (92.0)	1041.3 (93.0)	<0.001
RAnkle X, mean (SD)	541.0 (52.0)	514.3 (49.8)	<0.001	534.1 (65.8)	524.4 (59.6)	<0.001
RAnkle Y, mean (SD)	1324.1 (92.8)	1216.7 (87.0)	<0.001	1293.6 (111.1)	1155.3 (120.7)	<0.001
LAnkle X, mean (SD)	556.5 (36.7)	562.4 (34.9)	<0.001	563.5 (54.1)	564.8 (53.7)	0.446
LAnkle Y, mean (SD)	1323.6 (94.8)	1217.0 (86.4)	<0.001	1292.1 (113.6)	1152.7 (123.7)	<0.001
Chest, mean (SD)	933.6 (93.5)	808.5 (118.5)	<0.001	936.8 (110.8)	826.3 (142.9)	<0.001

the impact of each joint coordinate on foot position. The statistical significance of the results was evaluated using p-values. This evaluation provides valuable insights into how joint coordinates influence foot positioning during jump rope movements, which may improve the accuracy and efficiency of the exercise.

We conducted SHapley Additive exPlanations (SHAP) analysis to interpret the predictions of our best-performing model and to determine how much each joint coordinate contributed to these predictions. SHAP values quantify the impact of each feature, providing insights into which joint coordinates are most influential in determining jump rope execution performance. The summary plot displays the SHAP values for the 15 features that contribute the most to the model's predictions, with the absolute value of the SHAP value indicating feature importance. The color of the dots in the plot reflects the magnitude of the feature values, aiding in the understanding of each feature's impact. Additionally, the force plot visualizes SHAP values for specific data points, illustrating how each feature influences the model's predictions. In this plot, positive SHAP values are represented in red on the left, while negative values are shown in blue on the right, with the color intensity correlating to the magnitude of the feature values. This comprehensive analysis enhances our understanding of the factors affecting jump rope performance [21].

VI. EXPERIMENTAL RESULTS

We conducted a descriptive statistical analysis to evaluate whether there are statistically significant differences among the variables across classes, calculating p-values to assess the differences between groups. This process allowed us to confirm the mean, standard deviation, and statistical significance of the differences for each variable between the two groups. We determined that a variable had a statistically significant difference between the groups if the p-value was less than 0.05. As a result, all variables, except for the X coordinates of the left hip and the left elbow in the Double type, showed statistically significant differences between the two groups. The results are shown in Table 1, where the n indicates the number of frames corresponding to each class.

The results of the Pearson correlation analysis between joint coordinate data are presented in Table 2. The top 10 combinations with the highest positive correlations for both Single and Double types were visualized. The analysis revealed a strong positive correlation, with Pearson correlation coefficients close to 1, among the Y coordinates of the head, neck, chest, shoulders, wrists, hips, and elbows. The p-value indicates the probability that the correlation coefficient was observed by chance, and all the p-values for the correlation coefficients presented in the table were less than 0.001, confirming that the correlations are statistically significant and not due to random chance.

TABLE 2. Comparing pearson's correlation coefficients for single and double types.

Type							
Single				Double			
Feature 1	Feature 2	Pearson's r	p-value	Feature 1	Feature 2	Pearson's r	p-value
RShoulder Y	LShoulder Y	0.995	<0.001	RShoulder Y	LShoulder Y	0.994	<0.001
Head	Neck	0.994	<0.001	RHip Y	LHip Y	0.993	<0.001
Neck	LShoulder Y	0.994	<0.001	Neck	LShoulder Y	0.992	<0.001
Neck	RShoulder Y	0.994	<0.001	Head	Neck	0.991	<0.001
Head	LShoulder Y	0.990	<0.001	Neck	RShoulder Y	0.991	<0.001
Head	RShoulder Y	0.989	<0.001	Head	LShoulder Y	0.988	<0.001
RWrist Y	LWrist Y	0.988	<0.001	RShoulder Y	Chest	0.988	<0.001
RHip Y	LHip Y	0.987	<0.001	LShoulder Y	Chest	0.987	<0.001
RShoulder Y	Chest	0.979	<0.001	Head	RShoulder Y	0.987	<0.001
LShoulder Y	Chest	0.979	<0.001	RShoulder Y	RElbow Y	0.984	<0.001

TABLE 3. Comparing the performance of classification models.

Classification Models	Model Type	Type	Accuracy	Precision	Recall	F1 Score	Area under the Receiver Operating Characteristic Curve	Area under the Precision-Recall Curve
Random Forest [13]	Machine Learning	Single	0.784	0.784	0.784	0.783	0.886	0.856
		Double	0.887	0.888	0.887	0.886	0.952	0.946
Extra Trees [14]	Machine Learning	Single	0.774	0.775	0.774	0.773	0.878	0.844
		Double	0.889	0.889	0.889	0.888	0.945	0.945
Cat Boost [15]	Machine Learning	Single	0.782	0.782	0.782	0.782	0.864	0.797
		Double	0.897	0.898	0.897	0.897	**0.959**	0.962
Light GBM [16]	Machine Learning	Single	0.791	**0.791**	0.791	0.791	0.877	0.847
		Double	**0.899**	**0.903**	0.899	**0.898**	0.954	0.949
XG Boost [17]	Machine Learning	Single	0.774	0.774	0.774	0.773	0.863	0.811
		Double	0.886	0.888	0.886	0.885	**0.959**	**0.963**
LSTM [18]	Deep Learning	Single	0.798	0.779	0.786	0.782	0.841	0.706
		Double	0.870	0.862	**0.915**	0.888	0.953	0.959
Transformer [19]	Deep Learning	Single	**0.819**	0.789	**0.831**	**0.809**	**0.903**	**0.868**
		Double	0.831	0.822	0.891	0.855	0.933	0.949

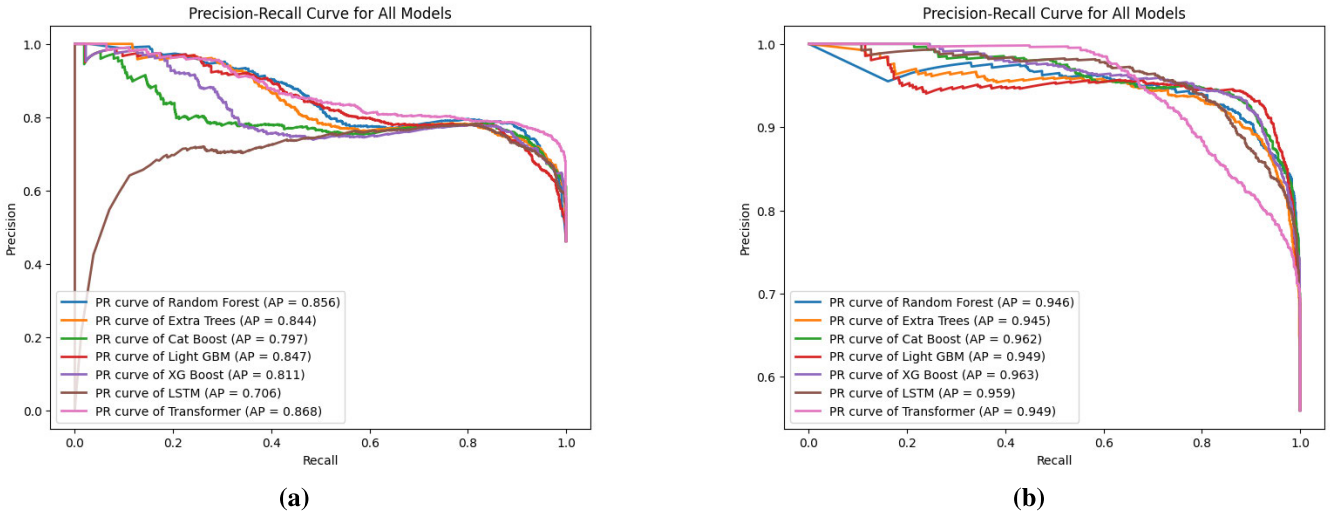

FIGURE 3. Precision-Recall curves for single and double types across seven models, (a) Single type, (b) Double type.

We used five tree-based machine learning models and two deep learning models to classify the foot's position using joint coordinate data. The performance measurement results for the test data are presented in Table 3. We conducted separate training for both Single type and Double type, using Accuracy, Precision, Recall, F1 score, AUROC, and AP as evaluation metrics. The comprehensive evaluation of the performance metrics showed that the Transformer model exhibited the best performance across all five evaluation metrics for Single type, making it the most suitable model for Single type measurement. For Double type, the LightGBM model demonstrated the best performance in three evaluation

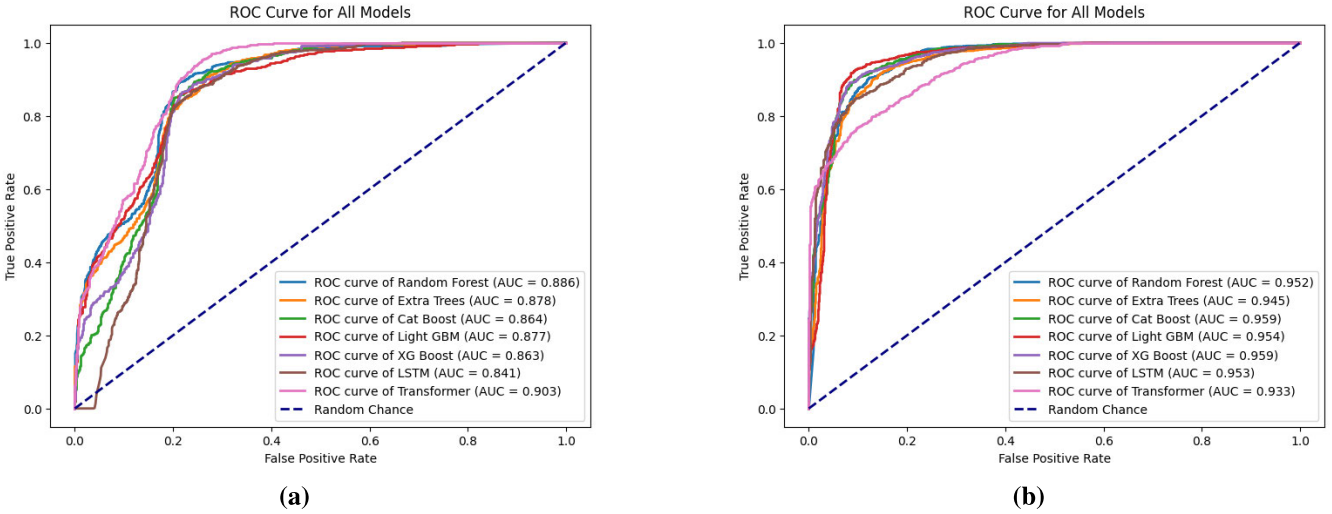

FIGURE 4. Receiver operating characteristic curves for single and double types across seven models, (a) Single type, (b) Double type.

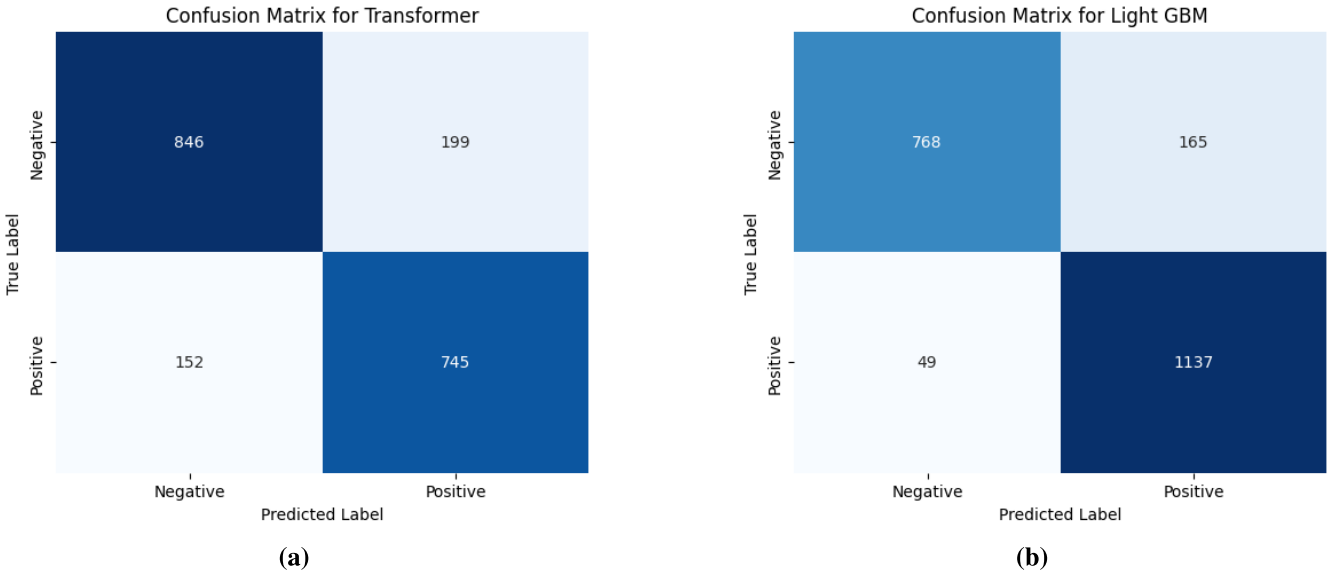

FIGURE 5. Confusion matrices for the best performing models, (a) Transformer for Single Type and (b) Light GBM for Double Type.

metrics, confirming it as the most suitable model for Double type measurement. In addition to these two models, overall performance was also satisfactory.

Figure 3 visualizes the Precision-Recall Curves for the seven models trained on the training data, showing the relationship between precision and recall for each model. Figure 4 displays the Receiver Operating Characteristic Curves for the same models, illustrating the relationship between the True Positive Rate and the False Positive Rate for each model.

Figure 5 visualizes the confusion matrices for the test data, showing the results of the Transformer model, which demonstrated the best performance for the Single type, and the Light GBM model, which showed the best performance for the Double type. The confusion matrix is an important metric for evaluating the classification performance of each model, representing the accurate classification results, including true positives, false positives, true negatives, and false negatives. The confusion matrices for the remaining models are visualized in Supplementary Material Fig. 1.

To assess the change in performance resulting from the application of the moving average, we visualized the model's prediction results before and after applying the technique. As shown in Fig. 6, the model initially predicted the number of jumps to be 13, whereas after applying the moving average, the prediction was accurately adjusted to 7.

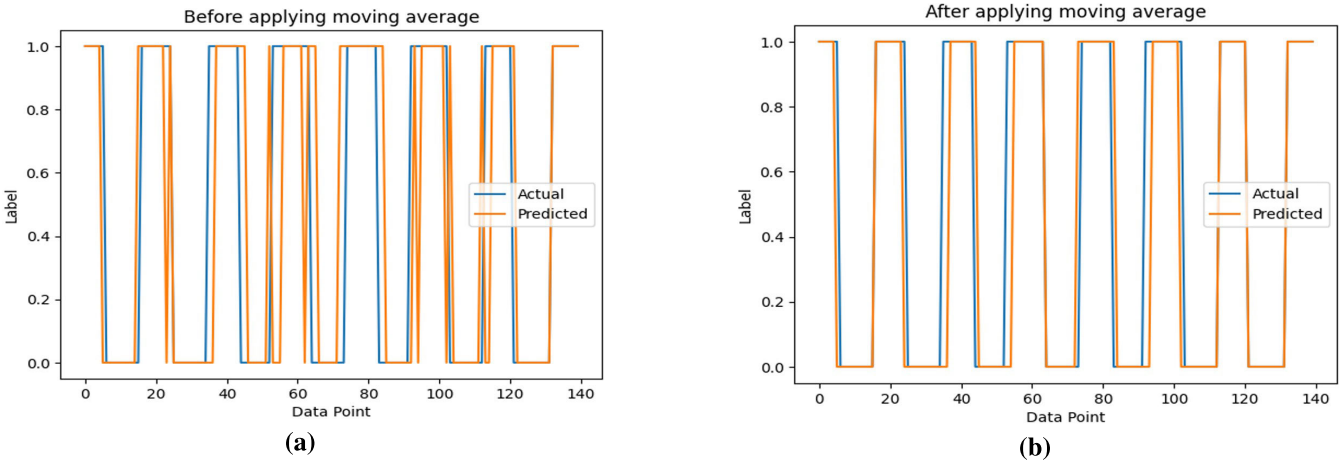

FIGURE 6. Comparison before and after applying moving average, (a) Before applying moving average and (b) After applying moving average.

TABLE 4. Significant odds ratios and 95% confidence intervals from logistic regression analysis for ten variables.

Type					
Single			Double		
Variable	Odds ratio (95% confidence interval)	P-value	Variable	Odds ratio (95% confidence interval)	P-value
RShoulder X	1.002 (0.994 - 1.010)	<0.001	Neck	1.024 (1.017 - 1.030)	<0.001
LShoulder X	0.957 (0.949 - 0.966)	<0.001	RShoulder X	1.032 (1.024 - 1.040)	<0.001
RElbow X	0.965 (0.956 - 0.974)	<0.001	RShoulder Y	0.981 (0.973 - 0.990)	<0.001
LWrist X	1.011 (1.008 - 1.015)	<0.001	RElbow Y	0.981 (0.974 - 0.988)	<0.001
LWrist Y	1.018 (1.012 - 1.024)	<0.001	LElbow Y	0.984 (0.977 - 0.990)	<0.001
RKnee X	1.032 (1.019 - 1.046)	<0.001	RWrist Y	1.019 (1.014 - 1.024)	<0.001
RAnkle Y	1.021 (1.016 - 1.028)	<0.001	LWrist Y	1.022 (1.017 - 1.027)	<0.001
LAnkle X	1.029 (1.018 - 1.040)	<0.001	RAnkle X	0.978 (0.971 - 0.986)	<0.001
LAnkle Y	0.987 (0.982 - 0.992)	<0.001	LShoulder Y	0.984 (0.975 - 0.992)	0.002
Chest	0.972 (0.961 - 0.983)	<0.001	LKnee Y	0.991 (0.987 - 0.996)	0.002

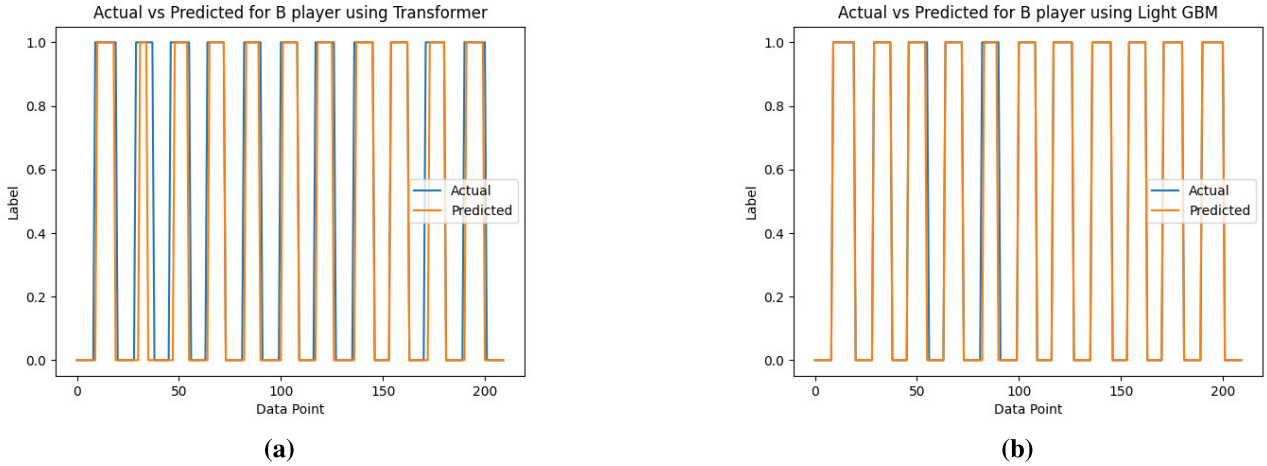

FIGURE 7. Visualization of predicted and actual values using transformer and LightGBM Models, (a) Transformer for Single Type, (b) LightGBM for Double Type.

To verify whether the jump rope count measurement was accurately performed, we visualized the predictions of each model using the Transformer, which showed the best performance for the Single type, and LightGBM, which demonstrated the best performance for the Double type. This was done for Performer B, who performed the Single type 11 times, and Performer C, who performed the Double type 11 times, as shown in Fig. 7. Upon examining the figure, we can see that both the Single type and Double type predictions exhibited slight temporal errors in the

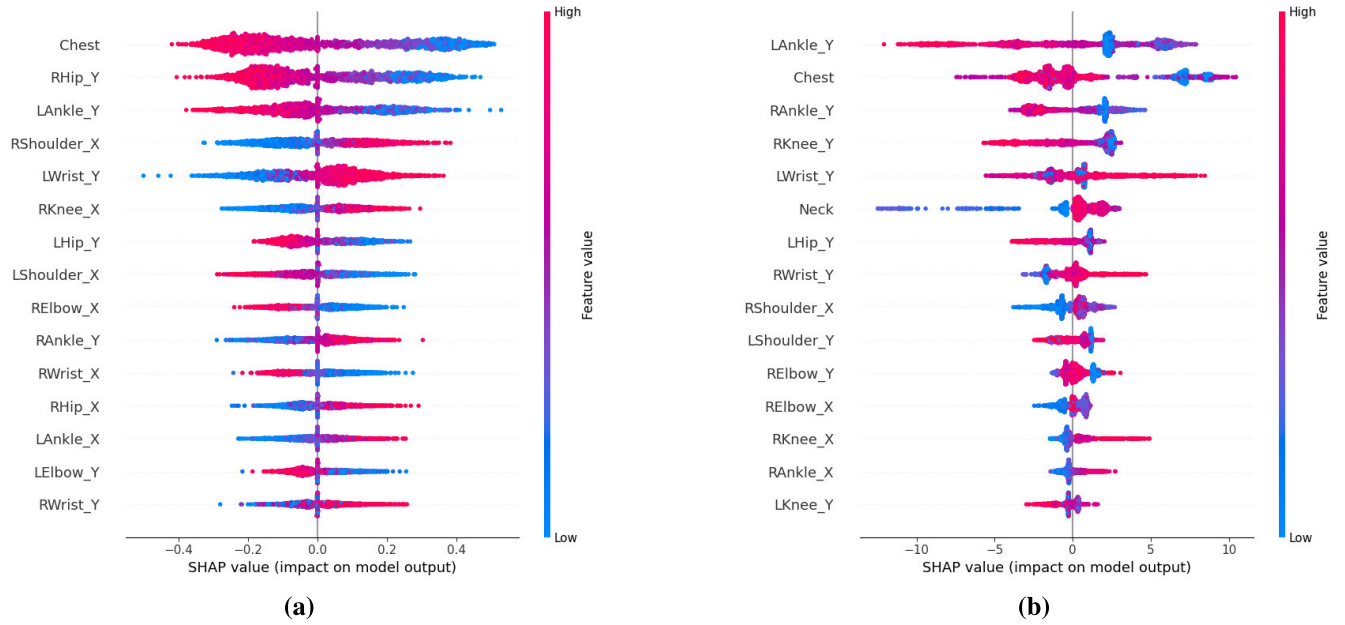

FIGURE 8. Summary plots for the transformer model for single type and the light GBM model for double type, (a) Transformer for Single Type, (b) Light GBM for Double Type.

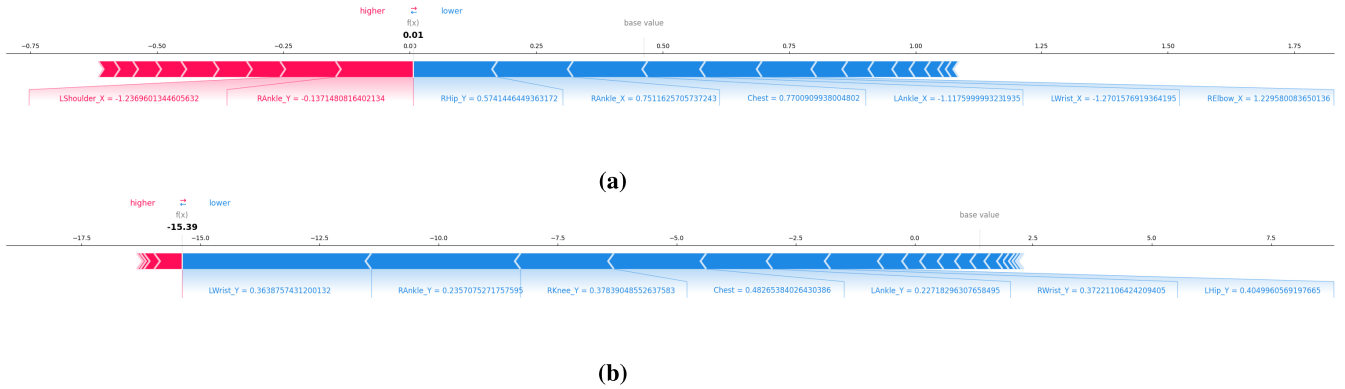

FIGURE 9. Force plots for the transformer model for single type and the light GBM model for double type, (a) Transformer for Single Type, (b) Light GBM for Double Type.

jump rope actions; however, the predicted count of 11 was accurate. Some of the prediction results for each performer using the seven models are visualized in Supplementary Material Fig. 2.

The results of the odds ratio analysis, as shown in Table 4, indicated that the single type, the X and Y coordinates of the left wrist, and the X coordinate of the left ankle increased the probability of the foot being airborne. Conversely, the X coordinate of the left shoulder and the X coordinate of the right elbow were found to increase the probability of the foot being on the ground, indicating that the foot's position may vary depending on the relative positions of the joints. In the case of the Double type, the coordinates of the neck and the X coordinate of the right shoulder increased the probability of the foot being airborne, while the Y coordinates of the right elbow and right shoulder increased the probability of the foot being on the ground. All p-values were below 0.002, confirming the statistical significance of the relationships and emphasizing that the odds ratios were not due to chance [20]. These findings highlight the importance of considering specific joint coordinates in the development of models for predicting foot position in future research.

We performed SHAP analysis on the Transformer model, which showed the best performance for the Single type, and the Light GBM model, which showed the best performance for the Double type. The results are visualized in the Summary plot in Fig. 8 and the Force Plot in Fig. 9, respectively.

In Figure 8, the Summary plot reveals that, for the Single type, the coordinates of the chest, right hip Y-coordinate, left ankle Y-coordinate, right shoulder X-coordinate, and

left wrist Y-coordinate significantly contribute to the classification of foot position. For the Double type, the left ankle Y-coordinate, chest, right ankle Y-coordinate, right knee Y-coordinate, and left wrist Y-coordinate also play important roles. In Figure 9, the Force plot illustrates the contributions of joint coordinates when the foot is in contact with the ground. In the Single type, the left hip Y-coordinate, right ankle X-coordinate, chest, and left ankle X-coordinate contribute to reducing the model's prediction value to 0. In contrast, for the Double type, the left wrist Y-coordinate, right ankle Y-coordinate, right knee Y-coordinate, and shoulder coordinates are confirmed to play critical roles in lowering the model's prediction value to 0. The summary plots and force plots for the remaining models are visualized in Supplementary Material Fig. 3 and 4, respectively.

VII. DISCUSSION

The MPII model was employed to extract joint coordinate data from each frame of the jump rope performance video, resulting in 27 joint coordinate data points obtained for each frame. However, slight missing values were observed in the wrist, shoulder, and elbow coordinates. Due to the dynamic nature of jump rope movements, the positions of these joints exhibited significant variation between frames. This outcome suggests that the MPII model may struggle to accurately detect these rapidly changing positions. Future research should consider alternative models or methods to improve sensitivity for these highly variable joints.

The Pearson correlation analysis revealed a strong positive correlation between the Y coordinates of the head, neck, chest, shoulders, wrists, hips, and elbows. Correlation coefficients close to 1 indicate that the movements of these joints are closely related, and this high positive correlation suggests that the positional changes of these joints are interrelated during the jump rope performance. All p-values for the correlation coefficients were below 0.001, confirming that the relationships observed are statistically significant and not due to chance [12].

According to the experimental results, the Transformer model recorded the highest performance in the classification of Single type, which may be due to the structural advantages of the Transformer in handling sequential data. For the Double type, the LightGBM model demonstrated the best performance across several evaluation metrics, suggesting that the boosted tree-based model might be more suitable for this type of data. The performance of each model was measured using metrics such as Accuracy, Precision, Recall, F1 score, AUROC, and AP, with both models showing high results in F1 score. Since all models were optimized through hyperparameter tuning, these results highlight the importance of selecting the appropriate model based on the data type. Future research could explore the possibility of improving performance through data expansion or by incorporating diverse algorithms.

We applied the moving average technique to the model's predictions to mitigate noise and improve accuracy. By smoothing the predicted values, we observed a significant enhancement in the model's performance, particularly regarding the counts of jump rope repetitions. The application of the moving average not only reduced the fluctuations caused by noise but also enabled a more reliable estimation of the target values. This improvement underscores the importance of post-processing techniques in enhancing model accuracy. Moreover, applying post-processing methods such as the moving average technique to the counts of other exercises with time series data, similar to jump rope, can yield more reliable results.

The results of the odds ratio analysis indicated that for the Single type, the X and Y coordinates of the left wrist and the X coordinate of the left ankle increased the probability of the foot being airborne. Conversely, the X coordinate of the left shoulder and the X coordinate of the right elbow were found to increase the probability of the foot being on the ground, indicating that the foot's position may vary depending on the relative positions of the joints. In the case of the Double type, the coordinates of the neck and the X coordinate of the right shoulder increased the probability of the foot being airborne, while the Y coordinates of the right elbow and right shoulder increased the probability of the foot being on the ground. All p-values were below 0.002, confirming the statistical significance of the relationships and emphasizing that the odds ratios were not due to chance [20]. These findings highlight the importance of considering specific joint coordinates in the development of models for predicting foot position in future research.

The results of the SHAP analysis indicate that for the Single type, the chest, the Y coordinate of the right hip, the Y coordinate of the left ankle, the X coordinate of the right shoulder, and the Y coordinate of the left wrist significantly contribute to the classification of foot position. For Double type, the Y coordinate of the left ankle, the chest, the Y coordinate of the right ankle, the Y coordinate of the right knee, and the Y coordinate of the left wrist were also confirmed to play important roles in foot position classification. The analysis of the force plot revealed that for Single type, the Y coordinate of the left hip, the X coordinate of the right ankle, the chest, and the X coordinate of the left ankle contributed to lowering the model's prediction value to 0. In contrast, for Double type, the Y coordinate of the left wrist, the Y coordinate of the right ankle, the Y coordinate of the right knee, and the coordinates of the shoulders played critical roles in reducing the model's prediction value to 0. These results emphasize that the relative position changes of each joint coordinate have a significant impact on whether the foot is in contact with the ground, suggesting that future research should refine the analysis of the contributions of these joint coordinates to develop models that accurately predict foot position.

VIII. CONCLUSION

We proposed a video-based jump rope assistance program that extracts joint coordinate data from jump rope

performance videos and measures the number of jumps by classifying foot positions. Additionally, we validated this classification using seven different models and gained insights into the influence of each joint coordinate on foot position classification through Pearson correlation analysis, odds ratio analysis, and SHAP analysis. This helped clarify how the relative positional changes of specific joints contribute to determining foot position.

We collected videos by directly filming 10 participants performing Single type and Double type jump rope activities for 3, 5, 7, 9, and 11 repetitions. Using the MPII model provided by the OpenPose library, we extracted 26 joint coordinates per frame from each jump rope video, resulting in one CSV file for each video, yielding a total of 100 joint coordinate datasets. To train the model, we labeled the last column of each dataset with 0 when the foot was in contact with the ground and 1 when the foot was airborne.

We conducted a Pearson correlation analysis to understand the interrelationships among joint coordinates during the jump rope performance and to analyze how the movement of specific joints affects the positional changes of other joints. The results indicated a strong positive correlation between the Y coordinates of the joints, with all correlation coefficients having p values below 0.001, confirm that these relationships are statistically significant.

We validated the classification of foot position based on joint coordinate data using five tree-based machine-learning models and two deep-learning models. The machine-learning models included Random Forest, Extra Trees, CatBoost, LightGBM, and XGBoost, while the deep learning models used were LSTM and Transformer. We employed evaluation metrics such as Accuracy, Precision, Recall, F1 score, AUC, and AP to assess each model's performance. The training for Single type and Double type was conducted separately. The experimental results indicated that considering the six evaluation metrics, the Transformer model demonstrated the the best performance for the Single type, while the LightGBM model achieved the highest performance for the Double type.

To enhance the accuracy of jump count predictions, we applied a moving average technique to the predictions to reduce noise and improve accuracy. By using the moving average, the predictions for the number of jumps became smoother and more reliable. This technique helped reduce variability caused by noise and enabled a more consistent estimation of the target values.

We conducted odds ratio analysis to examine the probability of foot position change. In the dataset, we labeled instances where the foot is on the ground as 0 and instances where the foot is in the air as 1, thus defining the occurrence of the foot being airborne as the event of interest. The odds ratio analysis revealed that for the Single type, the X and Y coordinates of the left wrist and the X coordinate of the left ankle increase the probability of the foot being airborne, while the X coordinate of the left shoulder and the X coordinate of the right elbow decreases this probability. For the Double type, increases in the X coordinates of the neck and right shoulder raise the probability of the foot being airborne, whereas the Y coordinates of the right elbow and right shoulder lower this probability. All p-values for these odds ratios were found to be below 0.002, supporting their statistical significance.

We conducted SHAP analysis to precisely assess the contributions of each joint coordinate to foot position classification, followed by visualizing the results with summary plots and force plots. The SHAP analysis revealed that for the Single type, the Y coordinates of the chest, right hip, left ankle, the X coordinate of the right shoulder, and the Y coordinate of the left wrist contributed most significantly to the top position classification. For the Double type, the Y coordinates of the left ankle, right ankle, right knee, and the Y coordinate of the left wrist was found to have the greatest impact on the foot position classification.

In future research, it will be necessary to expand the analysis to include a wider variety of movement types based on the current study results, as well as to collect additional jump rope performance data in different environments to enhance the model's generalization performance. Additionally, integrating other biometric signals such as heart and respiratory rates with joint coordinates could enable more comprehensive movement analysis. This approach could be applied not only to jump rope but also to other physical activities, contributing to the development of personalized exercise feedback systems. Adopting AIOps and AI platforms will improve the efficiency of data analysis and model operations while utilizing AI Serve will create an environment that provides real-time feedback to users. These integrated AI systems will enhance the accuracy of performance analysis and offer more effective personalized exercise solutions through real-time data processing and responsiveness [22]. Finally, to further improve the performance of machine learning and deep learning models, it is important to apply additional tuning and model ensemble techniques that consider more data and diverse features.

ETHICAL CONSIDERATIONS

This study was conducted in accordance with the Declaration of Helsinki. While ethical approval from an institutional review board was not obtained, informed consent was obtained from all participants prior to data collection.

REFERENCES

[1] Everyday Health. *Jump Rope Workouts: A Guide*. Accessed: Sep. 23, 2024. [Online]. Available: https://www.everydayhealth.com/fitness/jump-rope-workouts/guide/

[2] Korean Jump Rope Association. *Characteristics of Jump Rope Exercis*. Accessed: Sep. 23, 2024. [Online]. Available: https://www.jumprope.co.kr/room/feature.asp

[3] Z. Cao, G. Hidalgo, T. Simon, S.-E. Wei, and Y. Sheikh, "OpenPose: Realtime multi-person 2D pose estimation using part affinity fields," *IEEE Trans. Pattern Anal. Mach. Intell.*, vol. 43, no. 1, pp. 172–186, Jan. 2021, doi: 10.1109/TPAMI.2019.2929257.

[4] D. C. Jeong, H. Liu, S. Salazar, J. Jiang, and C. A. Kitts, "SoloPose: One-shot kinematic 3D human pose estimation with video data augmentation," 2023, *arXiv:2312.10195*.

[5] I. Korhonen, J. Parkka, and M. V. Gils, "Health monitoring in the home of the future," *IEEE Eng. Med. Biol. Mag.*, vol. 22, no. 3, pp. 66–73, Jul. 2003.
[6] K. Lorincz, B.-R. Chen, G. W. Challen, A. R. Chowdhury, S. Patel, P. Bonato, and M. Welsh, "Mercury: A wearable sensor network platform for high-fidelity motion analysis," in *Proc. 7th ACM Conf. Embedded Networked Sensor Syst.*, Nov. 2009, pp. 183–196.
[7] A. Pantelopoulos and N. G. Bourbakis, "A survey on wearable sensor-based systems for health monitoring and prognosis," *IEEE Trans. Syst., Man, Cybern., C*, vol. 40, no. 1, pp. 1–12, Jan. 2010.
[8] J.-M. Kim, J.-H. Han, and W.-H. Kim, "Skeleton image processing based fitness trainer mirror," in *Proc. KIIT Conf.*, 2020, pp. 605–607.
[9] K.-O. Kim, S.-Y. Oh, and R. Ha, "Work-out posture correction program development using deep learning," in *Proc. Korean Inf. Sci. Soc. Conf.*, 2021, pp. 1330–1332.
[10] H.-J. Choi, M.-G. Jeon, S.-H. Kim, S.-K. Ko, and H.-G. Jeong, "Deep learning-based workout classification and repetition counting using IMU sensor data," in *Proc. Symp. Korean Inst. Commun. Inf. Sci.*, 2022, pp. 961–962.
[11] H.-C. Lee and J.-J. Im, "Personal training using OpenPose," in *Proc. Conf. Korean Inst. Electr. Engineers (KIEE)*, 2023, pp. 2483–2484.
[12] K. Pearson, "Note on regression and inheritance in the case of two parents," *Proc. Roy. Soc. London*, vol. 58, pp. 240–242, Jan. 1895.
[13] L. Breiman, "Random forests," *Mach. Learn.*, vol. 45, pp. 5–32, Oct. 2001.
[14] P. Geurts, D. Ernst, and L. Wehenkel, "Extremely randomized trees," *Mach. Learn.*, vol. 63, no. 1, pp. 3–42, Apr. 2006.
[15] L. Prokhorenkova, G. Gusev, A. Vorobev, A. V. Dorogush, and A. Gulin, "CatBoost: Unbiased boosting with categorical features," 2017, *arXiv:1706.09516*.
[16] G. Ke, D. Wang, T. Chen, T. Wang, W. Chen, W. Ma, Q. Ye, and T. Y. Liu, "LightGBM: A highly efficient gradient boosting decision tree," in *Proc. Adv. Neural Inf. Process. Syst.*, vol. 30, 2017, pp. 3147–3155.
[17] T. Chen and C. Guestrin, "XGBoost: A scalable tree boosting system," in *Proc. 22nd ACM SIGKDD Int. Conf. Knowl. Discovery Data Mining*, Aug. 2016, pp. 785–794.
[18] S. Hochreiter and J. Schmidhuber, "Long short-term memory," *Neural Comput.*, vol. 9, no. 8, pp. 1735–1780, Nov. 1997.
[19] A. Vaswani, N. Shazeer, N. Parmar, J. Uszkoreit, L. Jones, A. N. Gomez, L. Kaiser, and I. Polosukhin, "Attention is all you need," 2017, *arXiv:1706.03762*.
[20] S. Sperandei, "Understanding logistic regression analysis," *Biochemia Medica*, vol. 24, no. 1, pp. 12–18, 2014.
[21] S. Lundberg and S.-I. Lee, "A unified approach to interpreting model predictions," 2017, *arXiv:1705.07874*.
[22] Microsoft. (2024). *Advancing Azure Service Quality With Artificial Intelligence: AIOps*. Microsoft Azure Blog. Accessed: Oct. 12, 2024. [Online]. Available: https://azure.microsoft.com/en-us/blog/advancing-azure-service-quality-with-artificial-intelligence-aiops/

JIN-WOONG KIM is currently pursuing the bachelor's degree with Hansung University, Seoul, South Korea. His research interests include medical big data analysis and medical image diagnosis.

JAE-WOO SHIN received the B.S. degree in business administration from Korea University, South Korea, the M.B.A. degree from Purdue University, and the Ph.D. degree in information systems from Yonsei University. He is currently a Professor with the Department of IT Business Administration, Hanshin University. His main research interests include digital convergence, e-business, AI and data analysis, smart grids, and IT policy management.

SEOUNG-HO CHOI received the B.S. and M.S. degrees from Hansung University, South Korea, in 2018 and 2020, respectively. He joined the College of Liberal Arts, Faculty of Basic Liberal Arts, Hansung University, in 2023, where he is currently an Assistant Professor.